UCSF
UC San Francisco Previously Published Works

Title

The Androgen-Regulated Protease TMPRSS2 Activates a Proteolytic Cascade Involving Components of the Tumor Microenvironment and Promotes Prostate Cancer Metastasis

Permalink

https://escholarship.org/uc/item/9vw6c6hn

Journal

Cancer Discovery, 4(11)

ISSN

2159-8274

Authors

Lucas, Jared M
Heinlein, Cynthia
Kim, Tom
et al.

Publication Date

2014-11-01

DOI

10.1158/2159-8290.cd-13-1010

Peer reviewed

The Androgen-Regulated Protease TMPRSS2 Activates aProteolytic Cascade Involving Components of the Tumor Microenvironment and Promotes Prostate Cancer Metastasis

Jared M. Lucas[1,*], **Cynthia Heinlein**[1,*], **Tom Kim**[1], **Susana A. Hernandez**[1], **Muzdah S. Malik**[1], **Lawrence D. True**[2], **Colm Morrissey**[3], **Eva Corey**[3], **Bruce Montgomery**[4], **Elahe Mostaghel**[1,4], **Nigel Clegg**[1], **Ilsa Coleman**[1], **Christopher M. Brown**[5], **Eric L. Schneider**[5], **Charles Craik**[5], **Julian Simon**[1], **Tony Bedalov**[1], and **Peter S. Nelson**[1,2,3,4,**]

[1]Divisions of Human Biology and Clinical Research, Fred Hutchinson Cancer Research Center, Seattle, WA 98109-1024

[2]Department of Pathology, University of Washington, Seattle, WA

[3]Department of Urology, University of Washington, Seattle, WA

[4]Department of Medicine, University of Washington, Seattle, WA

[5]Department of Pharmaceutical Chemistry, University of California San Francisco, San Francisco, CA, 94153

Abstract

TMPRSS2 is an androgen-regulated cell surface serine protease expressed predominantly in prostate epithelium. TMPRSS2 is expressed highly in localized high-grade prostate cancers and in the majority of human prostate cancer metastasis. Through the generation of mouse models with a targeted deletion of *Tmprss2*, we demonstrate that the activity of this protease regulates cancer cell invasion and metastasis to distant organs. By screening combinatorial peptide libraries we identified a spectrum of TMPRSS2 substrates that include pro-hepatocyte growth factor (HGF). HGF activated by TMPRSS2 promoted c-Met receptor tyrosine kinase signaling, and initiated a pro-invasive EMT phenotype. Chemical library screens identified a potent bioavailable TMPRSS2 inhibitor that suppressed prostate cancer metastasis *in vivo*. Together, these findings provide a mechanistic link between androgen-regulated signaling programs and prostate cancer metastasis that operate via context-dependent interactions with extracellular constituents of the tumor microenvironment.

Keywords

prostate cancer; protease; invasion; metastasis; androgen receptor

Address correspondence/reprint request to: Peter Nelson, M.D,. Division of Human Biology, Fred Hutchinson Cancer Research Center, Mailstop D4-100, 1100 Fairview Avenue, Seattle, WA 98105-1024, Phone: (206)-667-3377, Fax: (206)-667-2917, pnelson@fhcrc.org.
*These authors contributed equally to these studies.

Author Manuscript   Author Manuscript   Author Manuscript   Author Manuscript

INTRODUCTION

Proteolytic enzymes influence a diverse spectrum of biological processes integral to tumor growth and metastasis. Many features of cancer invasion parallel complex attributes of organogenesis that require orchestrated protease-mediated interactions with the extracellular environment. While early studies of protease activity in tumorigenesis focused on activities directed toward local structural barriers directly restraining tumor expansion, subsequent work has determined roles for proteases in all phases of tumor progression through mechanisms that involve the liberation and activation of growth factors, direct pro-invasive signaling through cell surface receptors, and the modification of distant metastatic site microenvironments.

Of the more than 170 human serine proteases identified to date, members of the small subfamily of type II transmembrane serine proteases (TTSPs) are of particular interest due to compartmentalized expression patterns localizing activity to a limited number of cell types, and demonstrated roles as direct contributors to cancer progression (1–3). TTSPs comprise a group of modular proteins that contain an N-terminal cytoplasmic domain of 20-60 amino acids, a transmembrane domain, and a variable array of domains that invariably includes an extracellular C-terminus comprising a serine protease catalytic triad (4). The most extensively studied member of the TTSP family, *matriptase/MT-SP1/ST14,* is overexpressed in several tumors of epithelial origin including carcinoma of the ovary, uterus, prostate, colon, cervix, and skin (reviewed in (5)), and is associated with poor outcomes in many studies of these malignancies. *hepsin/TMPRSS1* has been consistently shown to be overexpressed in prostate cancers at levels up to 30-fold over benign epithelium (6, 7). Overexpression of hepsin in murine prostate epithelium results in a disrupted basement membrane leading to weakened adhesion between epithelium and stroma. High levels of hepsin expression in the context of neoplastic transformation endows prostate tumors cells with the ability to complete the full metastatic process (8).

Transmembrane Protease Serine 2 (*TMPRSS2)* is a TTSP expressed in prostate epithelium and is upregulated in aggressive prostate cancers (9). TMPRSS2 is normally expressed several fold higher in the prostate relative to any other human tissue, though the normal physiological function(s) remains unknown. Importantly, unlike other TTSPs, TMPRSS2 transcription is regulated by androgenic ligands and the androgen receptor (AR) (10). This feature has been hypothesized to contribute to the high frequency of genomic rearrangements involving the TMPRSS2 promoter and members of the *ETS* gene family, particularly *ERG*, which places this oncogene under AR control(11, 12). Other than the contribution of TMPRSS2 regulatory sequences to these genomic rearrangements, the role(s) of TMPRSS2 in neoplasia has not been established.

In this study, we investigated the influence of TMPRSS2 on prostate carcinoma. We established that TMPRSS2 is consistently expressed at high levels in metastatic prostate cancers and is regulated by androgenic hormones *in vivo*. By developing mouse models with genetically altered Tmprss2 activity in the prostate, we determined that Tmprss2 promotes metastasis. Employing high-throughput screens of combinatorial peptide libraries we identified pro-hepatocyte growth factor (HGF) as a TMPRSS2 substrate and confirmed that

HGF and it's cognate receptor c-Met are activated in prostate cancers expressing TMPRSS2, a finding that also associated with the acquisition of a pro-invasive mesenchymal gene expression program. By screening small molecule libraries, we identified a bioavailable inhibitor of TMPRSS2 that suppressed prostate cancer metastasis. Together, these findings provide a mechanistic link between androgen-regulated signaling and prostate cancer metastasis that operates via interactions with components of the tumor microenvironment.

RESULTS

The TMPRSS2 protease is highly expressed in metastatic prostate cancers and is regulated by androgenic hormones in vivo

The TTSP family members hepsin and matriptase directly influence the invasive and metastatic capabilities of cancers arising in the prostate and other organs. Previous studies determined that these proteases, and the TTSP TMPRSS2, are elevated in localized prostate cancers (6, 9, 13). To directly compare the relative abundance of these highly similar proteases, we microdissected neoplastic epithelium from localized (n=14) and metastatic (n=40) prostate cancers and quantitated transcript levels incancer foci. We found that TMPRSS2 levels exceeded that of both hepsin and matriptase in the majority of prostate cancers evaluated (*p*<0.01 for all comparisons) (Fig. 1A, B). In accord with transcript levels, TMPRSS2 protein is elevated in primary cancers relative to benign epithelium (Fig. 1B), and localized to the luminal surface of benign polarized secretory epithelial cells, a location that excludes contact with basement membrane or stromal cells. In contrast, loss of basal epithelium in prostate cancer allows TMPRSS2-expressing invasive neoplastic cells to directly interact with structural and cellular constituents of prostatic stroma (Fig. 1B).

The presence of high TMPRSS2 levels in invasive prostate cancers prompted further investigation of TMPRSS2 in metastasis (Fig. 1C). Patients with advanced prostate cancer disseminate tumor cells to multiple distant sites, though predominantly to lymph node and bone. To assess the frequency and consistency of TMPRSS2 expression in metastatic cancer foci, we procured tumor tissue from at least 3 distinct foci from 44 men with metastatic disease. The vast majority (132 of 166) of metastasis to soft tissues and bone expressed high levels of the TMPRSS2 protein, and different metastasis from the same individual all generally exhibited concordant high (common) or low (rare) TMPRSS2 staining (Fig. 1D). Those few tumors with absent or very low TMPRSS2 expression were notable for low or absent AR expression. Though rearrangements involving TMPRSS2 and ERG are usually accompanied by loss of one TMPRSS2 allele, we found no significant differences in TMPRSS2 expression between tumors with high or low ERG expression (Fig. 1E, F). The consistent retention of high levels of TMPRSS2 in prostate cancer metastasis suggested that this protease may exert a functional role in tumor cell dissemination and survival in foreign sites.

TMPRSS2 expression is regulated by androgens in vivo

The cellular signaling program regulated by the AR is a primary target of prostate cancer therapies, though the critical AR-regulated effector components responsible for the genesis or progression of prostate cancer have not been defined. *In vitro* experiments determined

that TMPRSS2 expression is promoted through AR and potentially via estrogen receptor regulation (10, 14, 15). In support of these observations, we found a positive correlation between AR and TMPRSS2 in microdissected primary tumor epithelium (r^2=0.39; p<0.001). This positive correlation was also evident in metastatic castration-resistant human prostate cancers (CRPC), the majority of which exhibit AR signaling (r^2=0.37; p<0.001) (Supplementary Fig. S1A, B).

To further establish the role of AR in TMPRSS2 regulation *in vivo*, we quantitated TMPRSS2 transcripts in prostate epithelium in the context of pharmacological manipulation of the AR-axis. Men diagnosed with localized prostate adenocarcinoma were treated with the LHRH agonist leuprolide, or doses of estradiol sufficient to induce castrate serum levels of testosterone prior to radical prostatectomy. We isolated epithelial cells by laser-assisted microdissection and quantitated TMPRSS2 mRNAs by qRT-PCR. Compared to epithelium from untreated individuals, TMPRSS2 transcripts were significantly lower in men receiving leuprolide or estradiol (p<0.01) (Fig. 1G). In contrast, TMPRSS2 expression was not altered in tumor cells from men receiving cytotoxic chemotherapy (Supplementary Fig. S1C). We next confirmed the *in vivo* responsiveness of TMPRSS2 expression in the context of AR activity using the Lu-CaP35 xenograft model that regresses following castration (16). Over time, these xenografts develop a CRPC phenotype accompanied by reactivation of the AR signaling program. Using microdissection to directly compare equivalent cancer cell numbers in the xenografted tumors at different time points following castration, we found that TMPRSS2 is expressed highly in Lu-CaP35 tumor cells grown in eugonadal hosts, decreases at days 5 and 20 post-castration, and increases with the emergence of CRPC (Supplementary Fig. S1D).

TMPRSS2 promotes prostate cancer invasion and metastasis

The extracellular protease function predicted by the TMPRSS2 coding sequence coupled with findings of high TMPRSS2 levels in metastatic prostate cancers suggested a functional role for TMPRSS2 in the pathogenesis of prostate cancer metastasis. To test this hypothesis, we evaluated the contribution of Tmprss2 to the high frequency of metastasis observed in the *transgenic autochthonous mouse model for prostate cancer* (TRAMP) (17). We crossed TRAMP mice to astrain with a targeted deletion of the *Tmprss2* serine protease domain (18) and evaluated cohorts of *Tmprss2*$^{+/+}$; TRAMP and *Tmprss2*$^{-/-}$; TRAMP animals at 20 and 32 weeks of age. The frequency of primary prostate tumor development was not different between the two genotypes: 100% of the *Tmprss2*$^{+/+}$; TRAMP and *Tmprss2*$^{-/-}$; TRAMP animals developed prostate tumors grossly visible at necropsy (Fig. 2A). However, primary tumor sizes and weights in the strains were significantly different; at 32 weeks *Tmprss2*$^{+/+}$; TRAMP tumors averaged 2.65±0.65g while thosearising in *Tmprss2*$^{-/-}$; TRAMP animals were more than twice as large, averaging 6.39±1.24g (p=0.01 for difference) (Fig. 2B). Tumors in both strains were highly proliferative with Ki67 indices of 67% and 72% in *Tmprss2*$^{+/+}$ and *Tmprss2*$^{-/-}$ tumors, respectively (Supplementary Fig. S2A). Prostate neoplasms that develop in the TRAMP model are known to exhibit a histological spectrum of growth spanning hyperplasia to poorly differentiated carcinomas (19). At 32 weeks, neoplasms developing in both*Tmprss2*$^{-/-}$; TRAMP (n=17) and *Tmprss2*$^{+/+}$; TRAMP (n=16) strains exhibited a range of histological patterns with a tendency toward more poorly

differentiated tumors in the *Tmprss2*$^{-/-}$; TRAMP genotype, though this was not statistically significant (Supplementary Fig. S2B).

At necropsy, we evaluated each animal for the presence of metastasis both grossly and by tissue histology. At the 32-week time point, tumor cell dissemination to regional lymph nodes was common in both *Tmprss2*$^{+/+}$ (78%) and *Tmprss2*$^{-/-}$ (83%) backgrounds (*p*=0.6) (Fig. 2C). In contrast, the incidence of metastasis to distant solid organs was substantially lower in the TRAMP tumors arising in the *Tmprss2*$^{-/-}$ background. Of 18 *Tmprss2*$^{+/+}$; TRAMP animals examined, 11 had gross metastasis to solid organs such as the liver and lung (61%) while only 2 of 30 *Tmprss2*$^{-/-}$; TRAMP animals had macroscopically visible tumors (7%) with an additional 2 animals having microscopic foci in the liver (*p*=0.016) (Fig. 2C). The AR and Tmprss2 were expressed in primary tumors of both strains and inmetastatic*Tmprss2*$^{+/+}$; TRAMP tumor cells in liver and lung, though there were regions of metastasis with low to absent AR staining (Supplementary Fig. S2C–E).

Due to the germ-line *Tmprss2* loss-of-function mutation in the *Tmprss2*$^{-/-}$ strain, the elimination of Tmprss2 protease activity is not exclusive to prostate epithelium. To evaluate the possibility that Tmprss2 influences tumor dissemination through non-prostatic cell types, we excised primary tumors, dispersed the tumor cells, ensured cellular viability, and measured growth in semi-solid medium, and invasion through modified basement membrane by transwell assays. *Tmprss2*^{WT}; TRAMP tumor cells were substantially more capable of invasion than either benign epithelium or cells from TRAMP tumors lacking Tmprss2 protease (*p*<0.01) (Fig. 2D). We next introduced shRNAs targeting TMPRSS2 into LNCaP C4-2B cells and noted a significant reduction in cell proliferation and cell invasion compared to scrambled shRNA controls (*p*<0.001) (Supplementary Fig. S3A–B). Additionally, DU145 prostate cancer cells, a line that normally expresses no TMPRSS2, engineered to express wild-type TMPRSS2 were more capable of anchorage independent growth than vector control DU145 cells or those expressing a protease-dead mutant form of TMPRSS2, TMPRSS2^{PM} (Fig. 2E).

We next excised primary tumors from *Tmprss2*$^{+/+}$; TRAMP and *Tmprss2*$^{-/-}$; TRAMP strains, dissociated the tumors, and injected viable tumor cells into the tail vein of wild-type recipient mice (Fig. 2F). Using PCR to detect the presence of SV40T antigen as a surrogate for the presence of tumor cells, we assessed blood, liver and lung over a time course of 28 days. SV40T antigen was readily detectable in the blood and tissues of mice injected with *Tmprss2*$^{-/-}$; TRAMP tumor cells up to 30 minutes, and in blood up to 24 hours, after which the SV40T levels diminished markedly and were undetectable by day 14 (Fig. 2G). Non-viable tumor cells were rapidly cleared and undetectable after 4 hours (Supplementary Fig. S4A). In contrast, SV40T DNA was readily measureable in the lung and liver 3 days post*Tmprss2*$^{+/+}$; TRAMP tumor cell injection and remained detectable in these tissues until the time of necropsy at day 28 at which time gross metastasis were evident. Primary tumors resected from 5 different *Tmprss2*$^{+/+}$; TRAMP donor animals aged 32 weeks, produced grossly visible liver or lung metastasis in 21 of 21 recipients, while tumor cells derived from *Tmprss2*$^{-/-}$; TRAMP primary tumors failed to generate metastasis in any of 28 recipients (*p*<0.01) (Table 1 and Fig. 2H).

We next evaluated the capability of Tmprss2 to directly affect the survival and growth of prostate cancer cells in a distant site. The bone is a frequent location of prostate cancer metastasis in humans, though this predilection is poorly recapitulated in any spontaneous mouse model of prostate cancer for reasons that remain unclear. We injected cells directly harvested from 32 week *Tmprss2⁺/⁺; TRAMP* or *Tmprss2⁻/⁻; TRAMP* primary tumors into the tibia of recipient hosts. Mild radiographic abnormalities were noted in bone engrafted with *Tmprss2⁻/⁻*; TRAMP cells, but tumor growth or bone destruction was not evident (Supplementary Fig. S4B). Radiographs of bone engrafted with cells from *Tmprss2⁺/⁺*; TRAMP tumors demonstrated a marked expansile mass with mixed lytic and blastic features (Supplementary Fig. S4B). Histological examination determined that 21 of 32 (66%) recipients of tumor cells derived from 6 different 32-week *Tmprss2⁺/⁺; TRAMP* donors had tumors, while none were identified in 29 recipients of tumors cells from 8 different *Tmprss2⁻/⁻*; TRAMP donors ($p<0.001$). Two of seven animals with *Tmprss2⁺/⁺; TRAMP* tibial grafts where distant organs were examined also had liver metastasis. No distant metastasis were identified in mice grafted with cells from *Tmprss2⁻/⁻*; TRAMP tumors.

Identification of TMPRSS2 substrate specificity by Positional Scanning of Synthetic Combinatorial Peptide Libraries (PS-SCL)

To identify substrates of TMPRSS2 that could contribute to the metastatic phenotype we took an approach designed to establish a hierarchy of likely target proteins based on biochemically-defined cleavage specificity. To assess the primary (P1) and extended (P2–P4) TMPRSS2 cleavage sequence, we screened pools of synthetic peptides each with a structure of Ac-P4-P3-P2-P1-ACC (7-amino-4-carbamoylmethylcoumarin) (20, 21). We tested TMPRSS2 against 160,000 distinct peptides for proteolytic activity *in vitro*. At the P1 position, TMPRSS2 strongly preferred substrates with an arginine rather than a lysine (Fig. 3A). The P2–P4 specificity of TMPRSS2 is distinct from the optimal cleavage specificities defined for other extracellular serine proteases including hepsin, MT-SP1/matriptase, thrombin, plasmin, tryptases βI and βII, prostasin and KLK4 (Supplementary Fig. S5), but TMPRSS2 also exhibits a degree of overlap with hepsin and MTSP1 substrates (22–25). We next created a database of human sequences that contain a trypsin-like fold as extracted from Pfamand MEROPS databases. Based on the information obtained from the TMPRSS2 PS-SCL peptide profiling, we identified serine protease-fold like proteins that had (i) activation domains comprising a known or predicted P4–P1 sequence, (ii) P1 position comprised of arginine, and (iii) a P1′ position comprising a hydrophobic amino acid (isoleucine or valine) to bind to the large, hydrophobic S1 pocket of TMPRSS2 (Supplementary Fig. S6A–C).

Results of TMPRSS2 substrate screening identified the activation sequences PQFR in the zymogen precursors of tissue plasminogen activator (PLAT), and IQSR in human glandular kallikrein 2 (hK2). Of interest, both PLAT and hK2 participate in protease cascades culminating in the anti-coagulation of blood or seminal fluid, respectively (26, 27). We confirmed that TMPRSS2 proteolyzed pro-hK2 and exhibited no activity toward MMP2 and MMP9, proteins without predicted TMPRSS2 cleavage sites (Supplementary Fig. S7A–D). hK2 is produced by benign prostate epithelial cells and is secreted into the glandular lumen where it is known to activate prostate specific antigen (PSA), a protease that in turn lyses the procoagulant seminogelin seminal fluid proteins. These results indicate that TMPRSS2

participates in proteolytic cascades of relevance for the normal physiological function of the prostate.

TMPRSS2 activates hepatocyte growth factor, promotes signaling through c-Met, and engages a gene expression program contributing to metastasis

Results of TMPRSS2 substrate screening identified the peptide KQLR, a sequence identical to the activation sequence of the single chain precursor form of hepatocyte growth factor (HGF). HGF has structural similarity to serine-proteases, and functions as the ligand of the c-Met receptor tyrosine kinase (28). Several studies have shown that HGF and c-Met comprise a signaling pathway of relevance for prostate cancer invasion and metastasis (29, 30). Cleavage of the single chain HGF precursor by known activators such as HGFAC and matriptase, produce a functional $α/β$-heterodimeric HGF capable of engaging the c-Met receptor (31). To test whether TMPRSS2 could activate HGF we evaluated its proteolytic activity toward a preparation of precursor sc-HGF. Exposure to active TMPRSS2 resulted in the loss of detectable pro-scHGF (Fig. 3B), an observation not recapitulated following incubation with aprotease-inactive TMPRSS2 mutant or vehicle control. We next confirmed that TMPRSS2-processed HGF, $HGF_{TMPRSS2}$, activates the c-Met receptor. We exposed DU145 cells, known to express c-Met, with pro-HGF pre-incubated with matriptase, a known activator of HGF. Met activation was determined by demonstrating receptor phosphorylation (Fig. 3C). Exposure of these cells to pro-HGF alone did not result in detectable Met phosphorylation. However, pro-HGF activated by incubation with TMPRSS2 resulted in Met phosphorylation. The inclusion of anti-HGF neutralizing antibody eliminated Met phosphorylation, demonstrating that activation resulted from HGF (Fig. 3C). DU145 cells exposed to HGF proteolyzed by TMPRSS2 were substantially more invasive when compared to cells treated with mock-activated pro-HGF ($p<0.01$) (Fig. 4A). Invasion was blocked by an HGF neutralizing antibody. The addition of TMPRSS2 to conditioned medium from prostate fibroblasts also significantly increased the invasion of DU145 cells, an effect that was not observed with a TMPRSS2 protease mutant, or the addition of HGF neutralizing antibody or the c-Met inhibitor SU11274 (Fig. 4B). LNCaP and C4-2B cells that natively express TMPRSS2, and PC3 and DU145 cells engineered to express TMPRSS2 exhibited enhanced invasion when exposed to pro-HGF ($p<0.01$) (Fig. 4C–E and Supplementary Fig. S7E).

The unanticipated finding that primary tumors developing in $Tmprss2^{-/-}$; TRAMP mice were substantially larger than those arising in $Tmprss2^{+/+}$; TRAMP mice, yet possessed attenuated metastatic capabilities, prompted further studies to evaluate the role of HGF in this process. When exposed to HGF, DU145 cells increased rates of proliferation ($p<0.01$) (Fig. 4F). However, HGF suppressed the proliferation of TC2 cells, a line derived from a TRAMP tumor ($p<0.03$) (Fig. 4G), while still promoting invasion (Fig. 4H). Similarly, the proliferation of non-tumorigenic BPH1 cells was suppressed by HGF exposure (Fig. 4G). Consistent with these observations, TC2 cells exposed to HGF upregulated the expression of cell cycle inhibitors p21 and p27 with concomitant decreases in proliferating nuclear antigen (PCNA), whereas PCNA expression increased in DU145 cells (Fig. 4I, J). These studies demonstrate that HGF signaling can simultaneously suppress cell proliferation while enhancing invasive phenotypes.

As HGF signaling is known to promote a pro-metastatic epithelial to mesenchymal transition (EMT) (32, 33), we examined the expression of genes contributing to such a phenotype. We first confirmed that Tmprss2 and c-Met were expressed in primary and metastatic *Tmprss2$^{+/+}$; TRAMP* tumors (Fig. 5A). We next microdissected benign prostate epithelium from wild type animals, and neoplastic prostate epithelium from age-matched *Tmprss2$^{+/+}$; TRAMP* and *Tmprss2$^{-/-}$; TRAMP* strains. Microarray-based transcript profiling determined that genes associated with EMT are expressed at substantially higher levels in *Tmprss2$^{+/+}$; TRAMP* tumor cells relative to *Tmprss2$^{-/-}$; TRAMP* cells or benign epithelium (Fig. 5B, C). We confirmed increases in the mesenchymal marker vimentin (2.1-fold), and EMT-associated transcripts encoding Twist1 (5.7-fold) and Twist2 (1.7-fold) by qRT-PCR (Fig. 5D). HGF signaling has been shown to promote invasive phenotypes through transcriptional regulation of CXCL12/CXCR4 chemokine components (34). Tumors excised from the highly metastatic TRAMP strain expressed 15-fold higher levels of Cxcl12α (Fig. 5D), whereas *Tmprss2$^{-/-}$; TRAMP* cells expressed Cxcl12α at levels equivalent to benign epithelium. Immunohistochemical staining confirmed that *Tmprss2^{WT}*; TRAMP tumor cells express high levels of the EMT-associated proteins vimentin and N-cadherin, and reductions of both were apparent in tumors arising in the absence of Tmprss2 (Fig. 5E). These findings indicate that Tmprss2 influences an EMT phenotype associated with enhanced cellular motility, invasion, and metastasis (Fig. 5F).

Chemicallibrary screens identify bromhexine hydrochloride as a bioavailable TMPRSS2 inhibitor that suppresses metastasis

To identify inhibitors of TMPRSS2 that may be used directly in clinical studies or as lead compounds to develop targeted drugs, we screened several chemical libraries with active TMPRSS2 protease, the chromogenic TMPRSS2 peptide substrate Boc-Gln-Ala-Arg-MCA, and compound concentrations of 5 μmol/L. We have used a similar approach to identify inhibitors of the hepsin protease (35). As a measure of reproducibility, the Z′ score for this assay was 0.78. The chemical libraries included 1248 FDA approved compounds, a Chembridge library of 13920 compounds, and a Chem-Div library of 54720 compounds. These screens led to the identification of five chemicals that inhibit TMPRSS2 protease activityof which one, bromhexine hydrochloride (BHH) is an FDA approved ingredient in mucolytic cough suppressants (Fig. 6A), and four are known only by their chemical identification numbers or CAS identifiers (Supplementary Fig. S8A).

The identified inhibitors; BHH, 0591-5329, 4401-0077, 4554-5138 and 8008-1235 were used in titration assays to determine the IC50's toward TMPRSS2 which ranged from 0.75 μM for BHH to 2.68 μM for 8008-1235. Each compound exhibited strong specificity toward TMPRSS2 relative to the related hepsin and matriptase proteases (Fig. 6B). Bromhexine IC50's for hepsin and matriptase were 35μM and 58μM respectively and exceeded 100μM for trypsin and thrombin (Supplementary Fig. S8B–C).

We next confirmed that the identified inhibitors were able to block TMPRSS2's ability to activate pro-plasminogen activator (pro-PLAT) *in vitro*. Assays consisted of pre-incubation of recombinant active TMPRSS2 with each compound, followed by a two-hour incubation with recombinant pro-PLAT. At the IC50 concentrations, each compound substantially

suppressed TMPRSS2-mediated proteolysis of this putative physiological substrate (Fig. 6C).

Of the five TMPRSS2 inhibitors identified in the screens, only BHH has been available in sufficient quantities to allow for further *in vitro* and *in vivo* studies. We assessed the toxicity and effects of BHHon cellular phenotypes of proliferation and invasion using *in vitro* cell-based assays. No significant toxicity was observed over a 48-hour period exposing LNCaP, DU145, PC3, or HepG2 cells to BHH concentrations ranging from 0μM to 250μM (Fig. 6D and Supplementary Fig. S9A–B). Since we have shown that TMPRSS2 activates HGF and is involved in promoting cellular invasion and migration, we tested BHH for the effectiveness in preventing invasion in a matrigel based *in vitro* cell culture invasion assay. DU145 and PC3 cells engineered to express TMPRSS2 were substantially more invasive than vector control cells with either standard culture conditions or with the addition of HGF ($p<0.01$). BHH treatment significantly reduced the migration and invasion phenotypes promoted by HGF in both DU145^{TMPRSS2} and PC-3^{TMPRSS2} cells ($p<0.01$) (Fig. 6E, F). BHH also significantly attenuated HGF-induced invasion of LNCaP and C4-2B cells that natively express TMPRSS2 ($p<0.01$) (Supplementary Fig. 9C, D).

Given that BHH is an FDA approved compound that has been used widely with no substantial adverse effects, we undertook a series of *in vivo* studies. Wild-type C57BL/6 and TRAMP mice were treated three times per week by intraperitoneal injection of 30mg/kg of BHH, a dose equivalent to ~2% of the acute LD50 dose in the published rodent toxicity studies. Treatments began at 15 weeks, an age in which the TRAMP mice are expected to have PIN (prostatic intraepithelial neoplasia) and continued for approximately 20 weeks until an age when the majority develop metastatic disease. In wild-type mice, no systemic toxicities were observed and there were no anatomical or histological alterations in the prostate glands when compared to mice treated with DMSO vehicle. The prostate weights were not different (0.51g versus 0.56g; $p=0.55$). As expected, the prostates of the vehicle-treated TRAMP mice were significantly larger than those from vehicle treated wild type C57BL/6 mice (1.6g versus 0.56g; $p<0.001$) and the histology of mice with a TRAMP genotype comprised a range of hyperplasia to invasive carcinomas. Notably, the prostate glands of the TRAMP mice treated with BHH were generally substantially larger than vehicle-treated TRAMP mice (5.2±0.6g versus 1.6±0.3g; $p<0.01$) (Fig. 6G, H). Further, BHH treatment significantly reduced the incidence of distant metastasis to lung and liver sites from 55% in vehicle-treated animals to 20% with BHH ($p=0.04$) (Fig. 6H). Collectively, these findings phenocopy the observations made in the context of genetic Tmprss2 manipulation where *Tmprss2$^{−/−}$*; TRAMP mice had larger primary tumors but reduced metastasis compared to *Tmprss2$^{+/+}$*; TRAMP animals.

To further assess the effects of BHH on metastasis, we injected tumor cells freshly harvested from primary TRAMP tumors into the tail veins of recipient mice. BHH (30mg/kg) or 1% DMSO (vehicle control) was administered one day before tumor cell injection, on the day of tumor injection, and then 3 times per week for 8 weeks. At necropsy, 87% and 93% of vehicle-treated mice were found to have histologically-confirmed lung or liver metastasis, respectively. In contrast, mice treated with BHH had substantially fewer lung (33% vs 87%; $p<0.01$) and liver (27% versus 93%; $p<0.01$) tumors (Fig. 6I, J).

DISCUSSION

The vast majority of deaths attributable to prostate cancer result from metastasis. While strong evidence supports a central role for androgen receptor (AR)-directed signaling in promoting the survival and proliferation of prostate cancers, contributions of the AR program to the metastatic process have not been established. Here we demonstrate that TMPRSS2, a serine protease regulated through AR transactivation and expressed at consistently high levels in prostate cancer metastasis, is a potent activator of HGF. Through interactions with the c-Met receptor tyrosine kinase, HGF orchestrates well-described developmental programs and contributes to pathological processes including carcinogenesis (36). Of particular relevance to the present study, c-Met-regulated programs can endow neoplastic epithelial cells with migratory and invasive capabilities and facilitate the acquisition of phenotypes normally associated with mesenchymal lineages. Aberrant c-Met signaling has been shown to occur through mechanisms that include activating point mutations, genomic amplification, and the autocrine production of HGF by tumor cells (37). c-Met signaling is also promoted through paracrine interactions with HGF generated by constituents of the tumor microenvironment such as fibroblasts, endothelial cells and leukocytes (38). In this situation proHGF is converted to mature HGF by cell surface proteolysis (36). The sequestration of HGF by constituents of extracellular matrix, coupled with the limited capability of active HGF to diffuse through extracellular domains strongly favors c-Met signaling in cell types capable of establishing intimate spatial relationships juxtaposing cell surface localized proteases and receptor bound proHGF. Such a mechanism has been shown to occur in squamous cell carcinoma where the TMPRSS2 family member matriptase induces tumorigenesis through proteolytic conversion of proHGF, consequent activation of c-Met signaling, and engagement of the PI3K-Akt-mTOR pathway (39).

Several lines of clinical evidence support a central role for signaling networks operating to promote a metastatic cascade in prostate cancer that involve AR, TMPRSS2, HGF, and c-Met interactions. Both the native prostate stroma, and constituents of bone, particularly osteoblasts, are known to generate high levels of HGF (40, 41). Striking regressions of prostate bone metastasis have been documented in human clinical trials of the c-Met inhibitor cabozantinib (42). Engagement of c-Met signaling induces a pro-invasive epithelial-to-mesenchymal transition (EMT) accompanied by a switch from E-cadherin to N-cadherin expression. N-cadherin is highly expressed by a subset of human prostate cancers with invasive and metastatic capabilities (43). We found that loss of Tmprss2 expression in TRAMP prostate tumors attenuated their metastatic capabilities and was associated with marked reductions of N-cadherin protein. A plausible model linking these events involves the induction of TMPRSS2 expression by AR-regulated transcription with consequent TMPRSS2 proteolysis of paracrine proHGF. The resulting engagement of c-Met signaling induces an invasive phenotype involving the acquisition of mesenchymal characteristics marked by the switch to N-cadherin production. While the TRAMP model often develops neuroendocrine and poorly differentiated tumors accompanied by diminished AR activity with disease progression, early stage tumors exhibit robust AR expression and respond to androgen deprivation with tumor regression. Of relevance for the present observations, metastatic human prostate cancers can exist as mixed tumors with both AR-

positive and AR-negative cells and also as hybrid tumors with concurrent expression of the AR and neuroendocrine markers within the same tumor cells (44). In this context, AR$^+$TMPRSS2$^+$ cells may activate HGF to exert paracrine effects on nearby cells that lack AR or TMPRSS2 activity, but that express c-Met.

Although loss of Tmprss2 protease activity substantially attenuated metastasis, the localized tumors that arose in the absence of Tmprss2 were unexpectedly of substantially greater size. This observation divorces primary tumor growth from metastatic behavior, and though counterintuitive, the findings are concordant with emerging views of metastasis (45, 46). There is precedent for discordance between primary tumor size and metastatic capabilities involving pro-oncogenic signaling (47). Our results, invoking differential microenvironment HGF states based on TMPRSS2-mediated activation, are also consistent with well-documented dichotomous effects of HGF whereby proliferative versus growth suppressing effects occur depending on cell context (36). HGF has been shown to restrain the proliferation of benign prostate epithelial cells and enhance growth rates of malignant cells, while inducing the migration of both cell types (30). HGF-mediated growth inhibitory and stimulatory responses have also been observed in cells derived from breast, ovarian, and other neoplasms (36). The downstream molecular interactions and signaling networks dictating the divergent reactions to HGF/c-Met signaling remain to be clarified.

A reduction in the frequency of metastases was also achieved by pharmacologic inactivation of TMPRSS2 with bromhexine, an FDA approved drug. This result not only further validatesTMPRSS2 as a drug target but also offers an opportunity for clinical studies. The magnitude of the reduction in metastases with bromhexine was lower than observed by genetic ablation of TMPRSS2, which may reflect incomplete pharmacologic blockade of protease activity with the treatment schedule we employed. As bromhexine is orally bioavailable, more frequent oral dosing may allow more complete and protracted inactivation of the enzyme in eventual clinical trials.

In summary, this study supports a causal role for TMPRSS2 in modulating the metastatic behavior of prostate cancer. The elevated levels of TMPRSS2 expression in high-grade localized carcinomas, and in disseminated tumor cells, coupled with regulatory controls exerted through AR activity suggest that this protease could represent a key effector of androgen-driven prostate cancer progression. These results link the AR program to the metastatic phenotype through mechanisms that depend on interactions with constituents of the local and distant tumor microenvironment, and suggest that therapeutic approaches directed toward inhibiting TMPRSS2 may reduce the incidence or progression of metastasis in prostate cancer patients.

MATERIALS AND METHODS

Mouse strains and tissue analyses

All mouse studies were performed under IACUC-approved protocols. The generation and characterization of *Tmprss2*−/− and the TRAMP mice has previously been described (18) (17, 48). Hematoxylin and eosin (H&E) staining was performed on 5 μm sections from various organs and reviewed by two pathologists (F. V. L. and L.T.) without knowledge of

the genotype of the animals and evaluated in accordance with previously described TRAMP tumor pathology (19, 48). Additional details are provided in Supplemental Methods.

Gene expression assays

Laser assisted microdissection was used to capture prostate epithelia from the ventral and anterior prostatic lobes as previously described (49). Microarray hybridization and qRT-PCR were used to quantitate mRNA abundance as detailed in Supplemental Methods. Microarray data are accessible in GEO using accession GSE58822. Primer sequences and PCR conditions for the various genes analyzed are provided in Supplemental Methods.

Cell culture and phenotypic assays

Cell lines used in these studies were used within 6 passages of original receipt or authenticated by comparing transcript profiles with those generated from original stocks. Additional details are provided in Supplemental Methods. The TMPRSS2 coding sequence was cloned into the pCR2.1-TOPO vector following the manufacturers protocol (Invitrogen, Carlsbad, CA), transfected into prostate cancer cells, and stable cell lines generated under antibiotic selection as detailed in Supplemental Procedures. The effect of TMPRSS2 on prostate cancer cell proliferation was determined by measuring the growth rates of individually selected TMPRSS2 expressing cell line clones in triplicate in 6-well tissue culture plates. Cells were trypsinized, stained with trypan blue and counted every 2 days for 8 days. The number of metabolically active cells was measured every day for 8 days using the Celltiter 96 Cell Proliferation Assay from Promega (Madison, WI). Cell invasion assays were performed using the QCM 96-Well Invasion Assay from Chemicon (Temecula, CA). Anchorage-independent growth differences were assayed following the procedure of Arteaga, et al. (1988).

Metastasis and Xenograft Assays

Primary prostate tumors were removed from Tmprss2$^{-/-}$; TRAMP or Tmprss2^{WT}; TRAMP mice at 28–32 weeks of age and transferred into phenol red free RPMI with 10% fetal bovine serum and antibiotics. Part of each tumor was fixed or frozen for histological analysis. Tumor tissue was minced with scalpels and passed through a 100 μm cell strainer (BD Falcon). Live cell number was estimated by trypan blue exclusion using a hemocytometer. Approximately 5×10^5 live cells were injected into the tail vein of 6–8 week old male ICR SCID mice (Taconic). SCID recipients were euthanized 8 weeks after injection. Intratibial injection of primary tumor cells was performed essentially as previously described (50). Mice were euthanized 8 weeks after injection. Radiographic images were obtained using a Faxitron with Kodak minR2000 film.

TMPRSS2 Substrate Identification

The methods for Positional Scanning of Synthetic Combinatorial peptide Libraries (PS-SCLs) were performed as described previously (20) and specific details are provided in Supplemental Methods. To identify preferred protein substrates for TMPRSS2, we used the information obtained from the PS-SCL peptide profiling and the testing of individual peptide substrates to create a database of human sequences that contain a trypsin-like fold as

extracted from Pfamand MEROPS databases. Candidate proteins were clustered and ranked based on matches with the preferred amino acids at the P1-P4 positions. We then tested the ability of TMPRSS2 to cleave selected candidate substrates from each cluster such as the HGF precursor, PLAT and KLK2 using standard *in vitro* digests, PAGE, and western blotting as described in the Supplemental Methods.

In Vivo Assays of Bromhexine

Primary prostate tumors were removed from TRAMP mice and transferred into phenol red free RPMI with 10% fetal bovine serum and antibiotics. The tumors were minced with scalpels and passed three times through a 100 μm cell strainer (BD Falcon). Dissociated live cells were counted using trypan blue exclusion and a hemocytometer. Six to eight week old ICR SCID mice (Taconic) were administered either Bromhexine hydrochloride (30mg/Kg) or 1% DMSO (vehicle control) one day before 5×10^4 dissociated live TRAMP tumor cells were injected into their tail veins. Mice also received the drug treatment on the day of tumor injection and then every other day for 8 weeks at which point the animals were euthanized, necropsied and examined for tumor growth, paying specific attention to their livers, lungs and kidneys.

Supplementary Material

Refer to Web version on PubMed Central for supplementary material.

Acknowledgments

Abbreviations

TMPRSS2	Transmembrane Protease Serine 2
TTSP	type II transmembrane serine protease
HGF	hepatocyte growth factor
EMT	epithelial to mesenchymal transition
AR	androgen receptor
TRAMP	transgenic autochthonous mouse model for prostate cancer

References

1. Netzel-Arnett S, Hooper JD, Szabo R, Madison EL, Quigley JP, Bugge TH, et al. Membrane anchored serine proteases: a rapidly expanding group of cell surface proteolytic enzymes with potential roles in cancer. Cancer Metastasis Rev. 2003; 22:237–58. [PubMed: 12784999]

2. Hooper JD, Clements JA, Quigley JP, Antalis TM. Type II transmembrane serine proteases. Insights into an emerging class of cell surface proteolytic enzymes. J Biol Chem. 2001; 276:857–60. [PubMed: 11060317]

3. Szabo R, Bugge TH. Type II transmembrane serine proteases in development and disease. Int J Biochem Cell Biol. 2008; 40:1297–316. [PubMed: 18191610]

4. Szabo R, Wu Q, Dickson RB, Netzel-Arnett S, Antalis TM, Bugge TH. Type II transmembrane serine proteases. Thromb Haemost. 2003; 90:185–93. [PubMed: 12888865]

5. List K, Bugge TH, Szabo R. Matriptase: potent proteolysis on the cell surface. Mol Med. 2006; 12:1–7. [PubMed: 16838070]

6. Magee JA, Araki T, Patil S, Ehrig T, True L, Humphrey PA, et al. Expression profiling reveals hepsin overexpression in prostate cancer. Cancer Res. 2001; 61:5692–6. [PubMed: 11479199]

7. Dhanasekaran SM, Barrette TR, Ghosh D, Shah R, Varambally S, Kurachi K, et al. Delineation of prognostic biomarkers in prostate cancer. Nature. 2001; 412:822–6. [PubMed: 11518967]

8. Klezovitch O, Chevillet J, Mirosevich J, Roberts RL, Matusik RJ, Vasioukhin V. Hepsin promotes prostate cancer progression and metastasis. Cancer Cell. 2004; 6:185–95. [PubMed: 15324701]

9. Lucas JM, True L, Hawley S, Matsumura M, Morrissey C, Vessella R, et al. The androgen-regulated type II serine protease TMPRSS2 is differentially expressed and mislocalized in prostate adenocarcinoma. The Journal of pathology. 2008; 215:118–25. [PubMed: 18338334]

10. Lin B, Ferguson C, White JT, Wang S, Vessella R, True LD, et al. Prostate-localized and androgen-regulated expression of the membrane- bound serine protease TMPRSS2. Cancer Res. 1999; 59:4180–4. [PubMed: 10485450]

11. Tomlins SA, Rhodes DR, Perner S, Dhanasekaran SM, Mehra R, Sun XW, et al. Recurrent fusion of TMPRSS2 and ETS transcription factor genes in prostate cancer. Science. 2005; 310:644–8. [PubMed: 16254181]

12. Lin C, Yang L, Tanasa B, Hutt K, Ju BG, Ohgi K, et al. Nuclear receptor-induced chromosomal proximity and DNA breaks underlie specific translocations in cancer. Cell. 2009; 139:1069–83. [PubMed: 19962179]

13. Saleem M, Adhami VM, Zhong W, Longley BJ, Lin CY, Dickson RB, et al. A novel biomarker for staging human prostate adenocarcinoma: overexpression of matriptase with concomitant loss of its inhibitor, hepatocyte growth factor activator inhibitor-1. Cancer Epidemiol Biomarkers Prev. 2006; 15:217–27. [PubMed: 16492908]

14. Wang Q, Li W, Liu XS, Carroll JS, Janne OA, Keeton EK, et al. A hierarchical network of transcription factors governs androgen receptor-dependent prostate cancer growth. Mol Cell. 2007; 27:380–92. [PubMed: 17679089]

15. Setlur SR, Mertz KD, Hoshida Y, Demichelis F, Lupien M, Perner S, et al. Estrogen-dependent signaling in a molecularly distinct subclass of aggressive prostate cancer. J Natl Cancer Inst. 2008; 100:815–25. [PubMed: 18505969]

16. Corey E, Quinn JE, Buhler KR, Nelson PS, Macoska JA, True LD, et al. LuCaP 35: a new model of prostate cancer progression to androgen independence. The Prostate. 2003; 55:239–46. [PubMed: 12712403]

17. Greenberg NM, DeMayo F, Finegold MJ, Medina D, Tilley WD, Aspinall JO, et al. Prostate cancer in a transgenic mouse. Proc Natl Acad Sci U S A. 1995; 92:3439–43. [PubMed: 7724580]

18. Kim TS, Heinlein C, Hackman RC, Nelson PS. Phenotypic analysis of mice lacking the Tmprss2-encoded protease. Mol Cell Biol. 2006; 26:965–75. [PubMed: 16428450]

19. Shappell SB, Thomas GV, Roberts RL, Herbert R, Ittmann MM, Rubin MA, et al. Prostate pathology of genetically engineered mice: definitions and classification. The consensus report from the Bar Harbor meeting of the Mouse Models of Human Cancer Consortium Prostate Pathology Committee. Cancer Res. 2004; 64:2270–305. [PubMed: 15026373]

20. Harris JL, Backes BJ, Leonetti F, Mahrus S, Ellman JA, Craik CS. Rapid and general profiling of protease specificity by using combinatorial fluorogenic substrate libraries. Proc Natl Acad Sci U S A. 2000; 97:7754–9. [PubMed: 10869434]

21. Choe Y, Leonetti F, Greenbaum DC, Lecaille F, Bogyo M, Bromme D, et al. Substrate profiling of cysteine proteases using a combinatorial peptide library identifies functionally unique specificities. J Biol Chem. 2006; 281:12824–32. [PubMed: 16520377]

22. Backes BJ, Harris JL, Leonetti F, Craik CS, Ellman JA. Synthesis of positional-scanning libraries of fluorogenic peptide substrates to define the extended substrate specificity of plasmin and thrombin. Nat Biotechnol. 2000; 18:187–93. [PubMed: 10657126]

23. Matsumura M, Bhatt AS, Andress D, Clegg N, Takayama TK, Craik CS, et al. Substrates of the prostate-specific serine protease prostase/KLK4 defined by positional-scanning peptide libraries. The Prostate. 2005; 62:1–13. [PubMed: 15389820]

24. Herter S, Piper DE, Aaron W, Gabriele T, Cutler G, Cao P, et al. Hepatocyte growth factor is a preferred in vitro substrate for human hepsin, a membrane-anchored serine protease implicated in prostate and ovarian cancers. Biochem J. 2005; 390:125–36. [PubMed: 15839837]

25. Shipway A, Danahay H, Williams JA, Tully DC, Backes BJ, Harris JL. Biochemical characterization of prostasin, a channel activating protease. Biochem Biophys Res Commun. 2004; 324:953–63. [PubMed: 15474520]

26. Davie EW. A brief historical review of the waterfall/cascade of blood coagulation. J Biol Chem. 2003; 278:50819–32. [PubMed: 14570883]

27. Lilja H, Abrahamsson PA, Lundwall A. Semenogelin, the predominant protein in human semen. Primary structure and identification of closely related proteins in the male accessory sex glands and on the spermatozoa. J Biol Chem. 1989; 264:1894–900. [PubMed: 2912989]

28. Bottaro DP, Rubin JS, Faletto DL, Chan AM, Kmiecik TE, Vande Woude GF, et al. Identification of the hepatocyte growth factor receptor as the c-met proto-oncogene product. Science. 1991; 251:802–4. [PubMed: 1846706]

29. Zhang YW, Su Y, Lanning N, Gustafson M, Shinomiya N, Zhao P, et al. Enhanced growth of human met-expressing xenografts in a new strain of immunocompromised mice transgenic for human hepatocyte growth factor/scatter factor. Oncogene. 2005; 24:101–6. [PubMed: 15531925]

30. Gmyrek GA, Walburg M, Webb CP, Yu HM, You X, Vaughan ED, et al. Normal and malignant prostate epithelial cells differ in their response to hepatocyte growth factor/scatter factor. The American journal of pathology. 2001; 159:579–90. [PubMed: 11485916]

31. Shimomura T, Ochiai M, Kondo J, Morimoto Y. A novel protease obtained from FBS-containing culture supernatant, that processes single chain form hepatocyte growth factor to two chain form in serum-free culture. Cytotechnology. 1992; 8:219–29. [PubMed: 1368819]

32. Grotegut S, von Schweinitz D, Christofori G, Lehembre F. Hepatocyte growth factor induces cell scattering through MAPK/Egr-1-mediated upregulation of Snail. The EMBO journal. 2006; 25:3534–45. [PubMed: 16858414]

33. Thiery JP, Acloque H, Huang RY, Nieto MA. Epithelial-mesenchymal transitions in development and disease. Cell. 2009; 139:871–90. [PubMed: 19945376]

34. Tu H, Zhou Z, Liang Q, Li Z, Li D, Qing J, et al. CXCR4 and SDF-1 production are stimulated by hepatocyte growth factor and promote glioma cell invasion. Onkologie. 2009; 32:331–6. [PubMed: 19521120]

35. Chevillet JR, Park GJ, Bedalov A, Simon JA, Vasioukhin VI. Identification and characterization of small-molecule inhibitors of hepsin. Mol Cancer Ther. 2008; 7:3343–51. [PubMed: 18852137]

36. Jiang W, Hiscox S, Matsumoto K, Nakamura T. Hepatocyte growth factor/scatter factor, its molecular, cellular and clinical implications in cancer. Crit Rev Oncol Hematol. 1999; 29:209–48. [PubMed: 10226727]

37. Boccaccio C, Comoglio PM. Invasive growth: a MET-driven genetic programme for cancer and stem cells. Nature reviews Cancer. 2006; 6:637–45.

38. Straussman R, Morikawa T, Shee K, Barzily-Rokni M, Qian ZR, Du J, et al. Tumour micro-environment elicits innate resistance to RAF inhibitors through HGF secretion. Nature. 2012; 487:500–4. [PubMed: 22763439]

39. Szabo R, Rasmussen AL, Moyer AB, Kosa P, Schafer JM, Molinolo AA, et al. c-Met-induced epithelial carcinogenesis is initiated by the serine protease matriptase. Oncogene. 2011; 30:2003–16. [PubMed: 21217780]

40. Weimar IS, Miranda N, Muller EJ, Hekman A, Kerst JM, de Gast GC, et al. Hepatocyte growth factor/scatter factor (HGF/SF) is produced by human bone marrow stromal cells and promotes proliferation, adhesion and survival of human hematopoietic progenitor cells (CD34+). Exp Hematol. 1998; 26:885–94. [PubMed: 9694510]

41. Knudsen BS, Gmyrek GA, Inra J, Scherr DS, Vaughan ED, Nanus DM, et al. High expression of the Met receptor in prostate cancer metastasis to bone. Urology. 2002; 60:1113–7. [PubMed: 12475693]

42. Gordon MS, Vogelzang NJ, Schoffski P, Daud A, Spira AI, O'Keeffe BA, et al. Activity of cabozantinib (XL184) in soft tissue and bone: Results of a phase II randomized discontinuation trial (RDT) in patients (pts) with advanced solid tumors. Journal of Clinical Oncology. 2011; 29:3010.

43. Tanaka H, Kono E, Tran CP, Miyazaki H, Yamashiro J, Shimomura T, et al. Monoclonal antibody targeting of N-cadherin inhibits prostate cancer growth, metastasis and castration resistance. Nature medicine. 2010; 16:1414–20.

44. Beltran H, Tomlins S, Aparicio A, Arora V, Rickman D, Ayala G, et al. Aggressive variants of castration-resistant prostate cancer. Clinical cancer research: an official journal of the American Association for Cancer Research. 2014; 20:2846–50. [PubMed: 24727321]

45. Chiang AC, Massague J. Molecular basis of metastasis. The New England journal of medicine. 2008; 359:2814–23. [PubMed: 19109576]

46. Weinberg RA. Leaving home early: reexamination of the canonical models of tumor progression. Cancer Cell. 2008; 14:283–4. [PubMed: 18835030]

47. Hutchinson JN, Jin J, Cardiff RD, Woodgett JR, Muller WJ. Activation of Akt-1 (PKB-alpha) can accelerate ErbB-2-mediated mammary tumorigenesis but suppresses tumor invasion. Cancer Res. 2004; 64:3171–8. [PubMed: 15126356]

48. Kaplan-Lefko PJ, Chen TM, Ittmann MM, Barrios RJ, Ayala GE, Huss WJ, et al. Pathobiology of autochthonous prostate cancer in a pre-clinical transgenic mouse model. The Prostate. 2003; 55:219–37. [PubMed: 12692788]

49. Pritchard C, Mecham B, Dumpit R, Coleman I, Bhattacharjee M, Chen Q, et al. Conserved gene expression programs integrate mammalian prostate development and tumorigenesis. Cancer Res. 2009; 69:1739–47. [PubMed: 19223557]

50. Corey E, Quinn JE, Bladou F, Brown LG, Roudier MP, Brown JM, et al. Establishment and characterization of osseous prostate cancer models: intratibial injection of human prostate cancer cells. The Prostate. 2002; 52:20–33. [PubMed: 11992617]

SIGNIFICANCE

The vast majority of prostate cancer deaths are due to metastasis. Loss of TMPRSS2 activity dramatically attenuated the metastatic phenotype through mechanisms involving the HGF/c-MET axis. Therapeutic approaches directed toward inhibiting TMPRSS2 may reduce the incidence or progression of metastasis in prostate cancer patients.
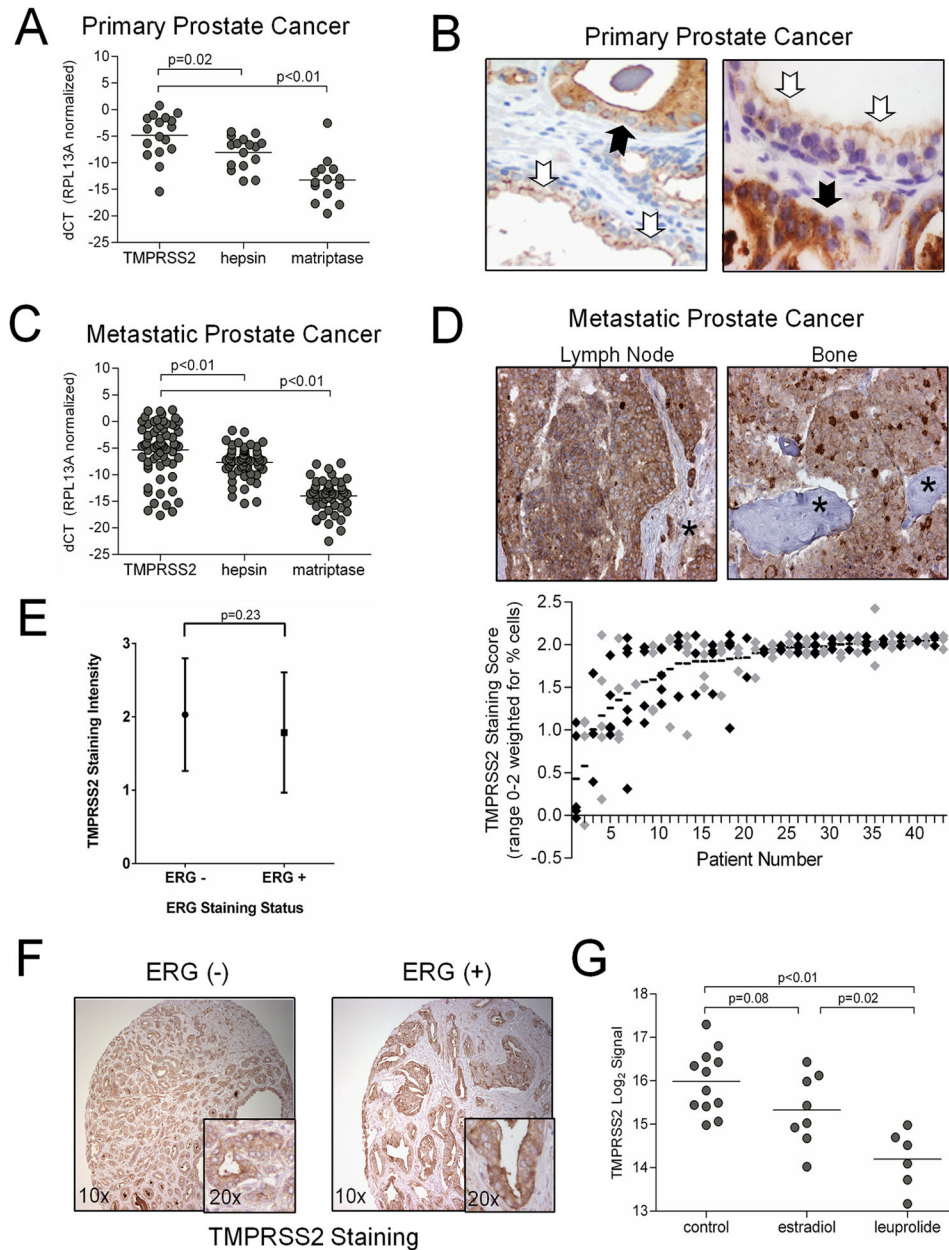
Figure 1. Expression of TMPRSS2 in prostate carcinoma

(A, C) qRT-PCR measurements of TMPRSS2, hepsin and matriptase mRNA from microdissected primary prostate carcinoma and metastasis from men with advanced CRPC. **(B)** Immunohistochemical localization of TMPRSS2 protein in benign prostate epithelium (white arrows) and prostate carcinoma (black arrows). TMPRSS2 in benign epithelium is oriented to the ductal lumen with little protein in contact with stromal constituents. In contrast, cancer cells expressing TMPRSS2 are in direct contact with stroma. **(D)** TMPRSS2 proteinin prostate cancer metastasis. Lymph node stroma and osteoid are denoted by an asterix. The consistency of TMPRSS2 protein in multiple different metastases from 44 patients with advanced prostate cancer demonstrates that most metastatic foci express

TMPRSS2 with a general concordance in multiple tumors from the same individual. Each data point represents an individual tumor focus and black (odd numbered patients) and gray (even numbered patients) data points alternate for clarity. (**E**) TMPRSS2 protein staining intensity in ERG positive versus ERG negative primary prostate cancers. (**F**) Representative example of TMPRSS2 protein expression in primary prostate cancers with or without ERG expression (**G**) Expression of TMPRSS2 in human prostate epithelium is attenuated following treatment with androgen-suppressing therapeutics, estradiol or the LHRH agonist leuprolide, compared to untreated controls.
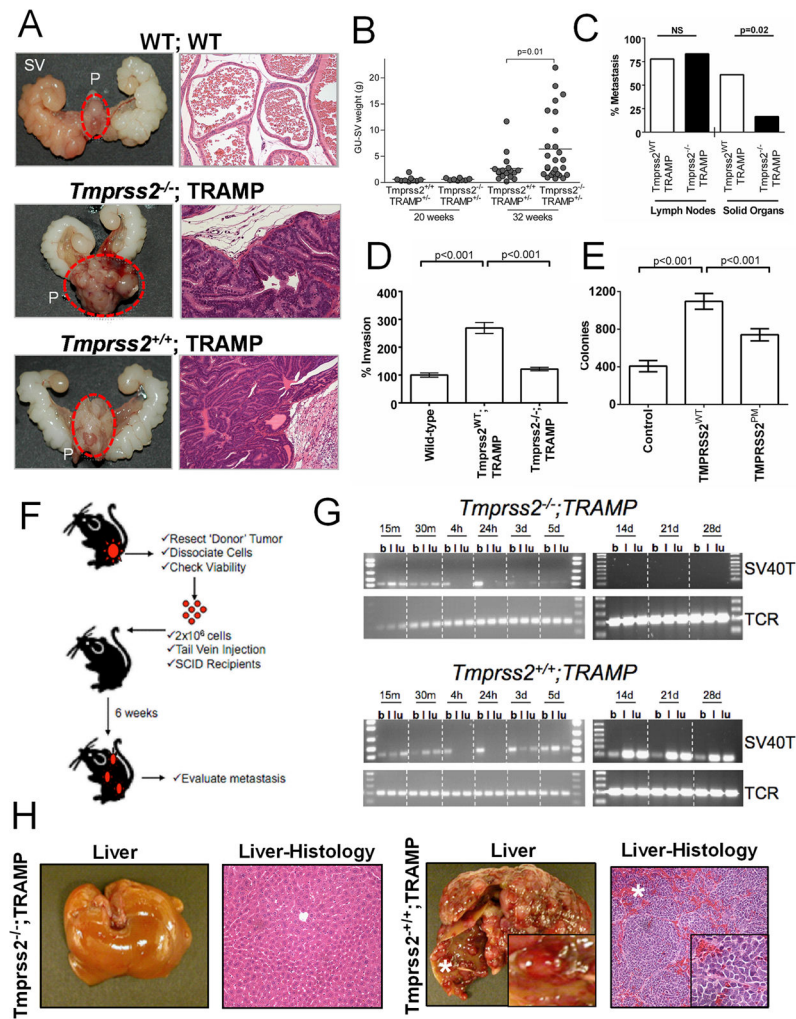
Figure 2. Tmprss2 influences prostate cancer growth and the development of metastasis
(A) Representative anatomical and histological images of prostate glands from wild type
(*WT; WT*) and TRAMP mice with (*Tmprss2*$^{+/+}$; TRAMP) and without (*Tmprss2*$^{-/-}$;
TRAMP) Tmprss2 protease activity. Both TRAMP genotypes exhibited a spectrum of well-
to poorly-differentiated carcinomas. P, prostate gland; SV, seminal vesicle. Prostate glands
are circled. **(B)** Weights of the genitourinary tracts (GU-SV) excised from TRAMP mice
with (*Tmprss2*$^{+/+}$; TRAMP) or without (*Tmprss2*$^{-/-}$; TRAMP) Tmprss2 activity. At 32
weeks of age, prostate tumors in *Tmprss2*$^{-/-}$; TRAMP mice were substantially larger than
those tumors excised from *Tmprss2*$^{+/+}$; TRAMP animals (*P*=0.01). **(C)** The frequency of
lymph node metastasis in *Tmprss2*$^{-/-}$; TRAMP versus *Tmprss2*$^{+/+}$; TRAMP genotypes was
similar. The frequency of metastasis to solid organs in TRAMP mice with inactive Tmprss2
was significantly reduced compared to TRAMP mice with wild-type Tmprss2 (*P*=0.02). **(D)**
Basement membrane invasion assays demonstrating enhanced invasion of primary cells
from *Tmprss2*^{WT}; TRAMP tumors relative to benign epithelium or primary tumor cells
deficient in Tmprss2 activity (*Tmprss2*$^{-/-}$; TRAMP). **(E)** Soft-agar colony formation assay
demonstrating enhanced anchorage-independent growth of DU145 prostate cancer cells
expressing wild-type active human TMPRSS2 (TMPRSS2^{WT}) versus a vector control or

protease-dead TMPRSS2 mutant (TMPRSS2^{PM}). **(F)** Schematic of the metastasis assay: primary tumors developing in *Tmprss2$^{-/-}$*; TRAMP or *Tmprss2$^{+/+}$*; TRAMP were resected, cells dissociated, and injected into tail veins of recipient hosts. **(G)** Detection of S40T antigen by PCR in blood (b), liver (l) or lung (lu) of mice at designated time points following tail-vein injections with primary prostate tumor cells from *Tmprss2$^{+/+}$*; TRAMP or *Tmprss2$^{-/-}$*; TRAMP mice. TCR, T-cell receptor.**(H)** Representative anatomical and histological images of livers from mice receiving vascular injections of cells from *Tmprss2$^{-/-}$*; TRAMP and*Tmprss2$^{+/+}$*; TRAMP tumors.
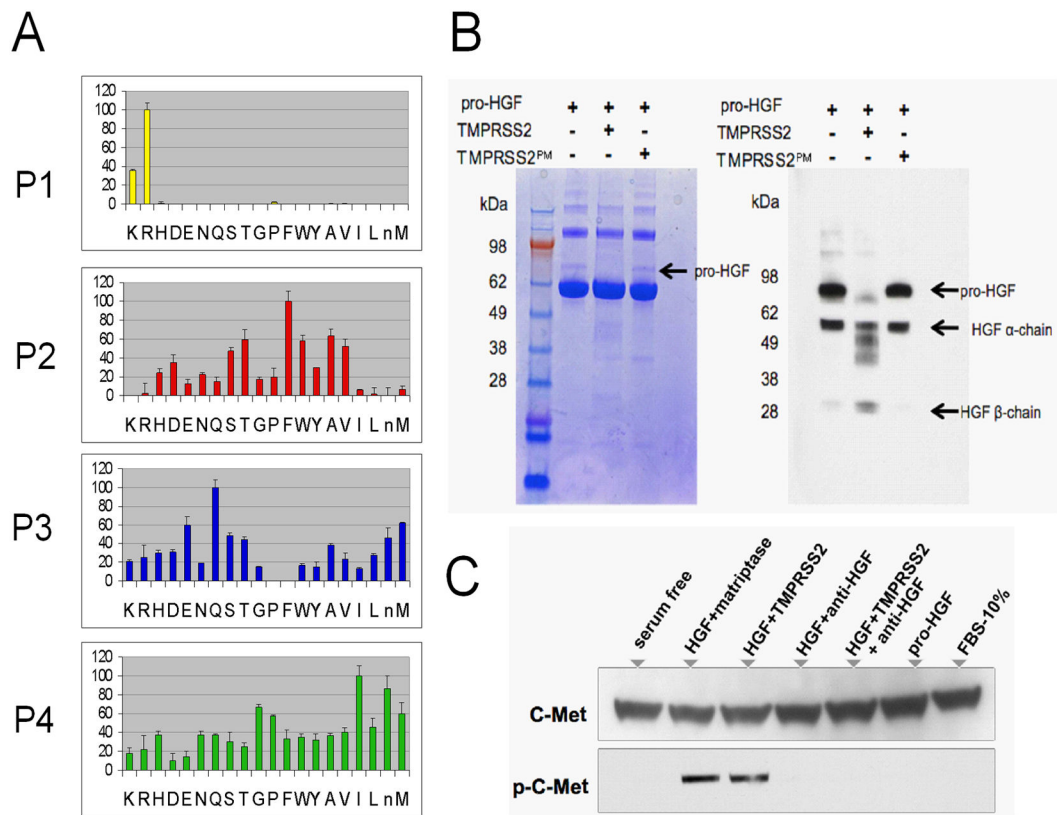
Figure 3. Identification of TMPRSS2 protease substrates
(A) Results of positional scanning of synthetic combinatorial peptide libraries (PS-SCL). The amino acid cleavage preferences are: P1 (R); P2 (T, F, W, A, V); P3 (E, M, Q); P4 (G, I, M). **(B)** pro-HGF is a substrate for TMPRSS2. The arrow denotes the single-chain (pro-) HGF and is not visualized following incubation with active TMPRSS2. The inactive TMPRSS2 protease-dead mutant (TMPRSS2^{PM}) is incapable of catalyzing HGF proteolysis. TMPRSS2 does not degrade the BSA carrier protein (dominant bands). Western blot analysis using a polyclonal anti-HGF antibody that recognizes multiple epitopes in the α and β chains of HGF demonstrates the loss of single chain (pro) HGF following incubation with active TMPRSS2 (lane 2), but not protease-dead TMPRSS2 (lane 3). **(C)** pro-HGF proteolyzed by TMPRSS2 activates c-Met as determined by immunodetection of phosphorylated c-Met (p-cMet) in DU145 prostate cancer cells. Control reactions with matriptase also demonstrate c-Met activation. Pro-HGF alone and the addition of anti-HGF neutralizing antibody abolishes c-Met phosphorylation.
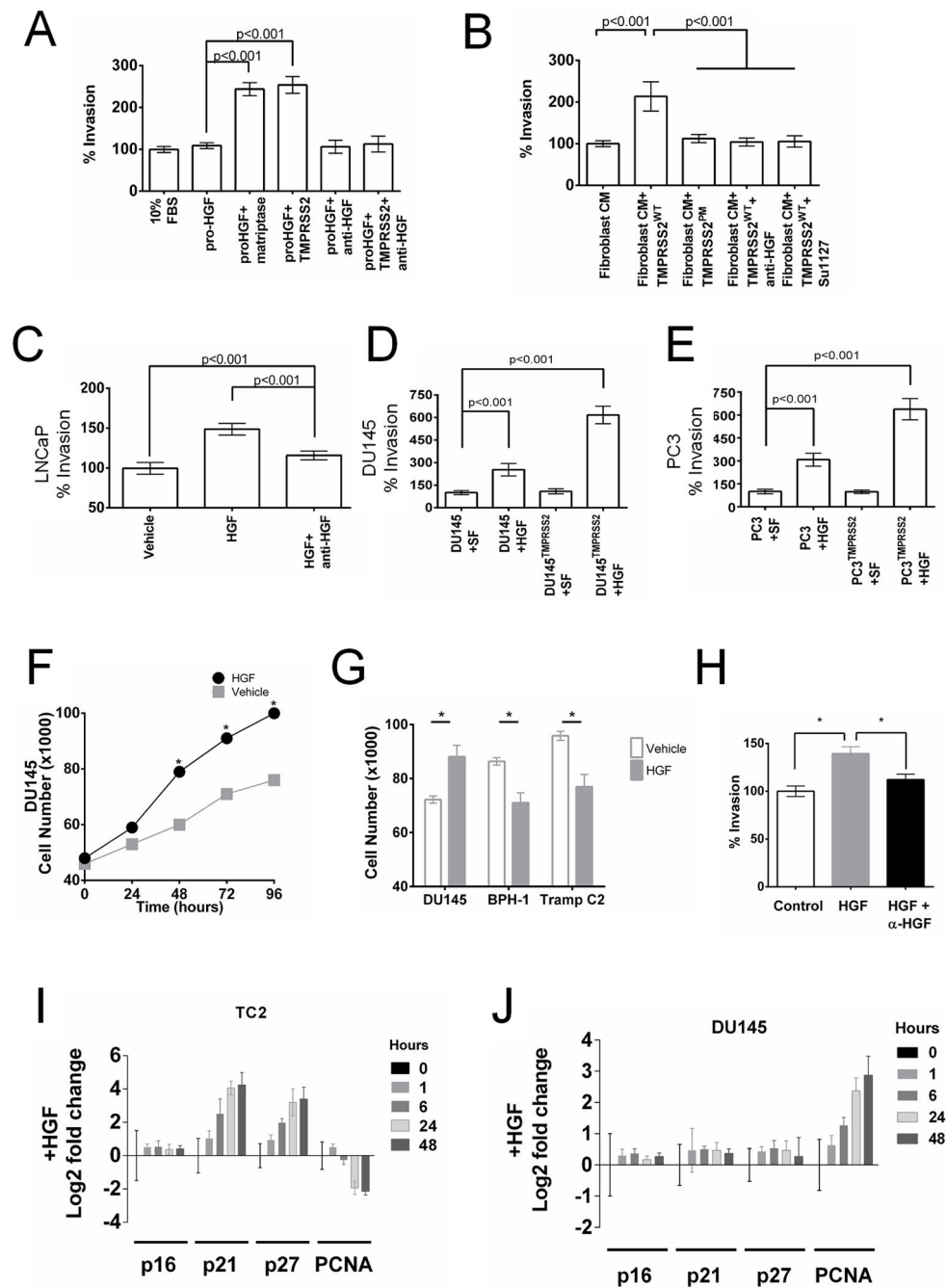
Figure 4. TMPRSS2-activated HGF consistently promotes invasion but differentially enhances or suppresses proliferation

(A) Exposure of DU145 prostate cancer cells to pro-HGF activated by either TMPRSS2 or matriptase increases cellular invasion. **(B)** Exposure of DU145 prostate cancer cells to prostate fibroblast conditioned medium and TMPRSS2 increases cellular invasion, which is not observed with an inactive TMPRSS2 protease mutant (TMPRSS2PM) and abolished with the addition of anti-HGF neutralizing antibody or the cMet inhibitor SU11274. The pro-invasive phenotype associated with TMPRSS2 expression in LNCaP **(C)** PC3 **(D)** and

DU145 **(E)** cells is promoted by exogenous paracrine-acting HGF. SF is serum-free medium. **(F, G)** TMPRSS2-activated HGF enhances the proliferation of DU145 cells and suppresses the proliferation of BPH1 and TRAMP C2 cells (TC2). Cell numbers were determined at 96 hours and represent a mean of 3 replicates (asterix = $p<0.01$). **(H)** Invasion of TRAMP C2 cells is promoted by TMPRSS2-activated HGF and attenuated with anti-HGF neutralizing antibody (asterix = $p<0.01$). Differential effects of activated HGF on cell cycle regulators p21 and p27 in TC2 **(I)** and DU145 **(J)** cells.
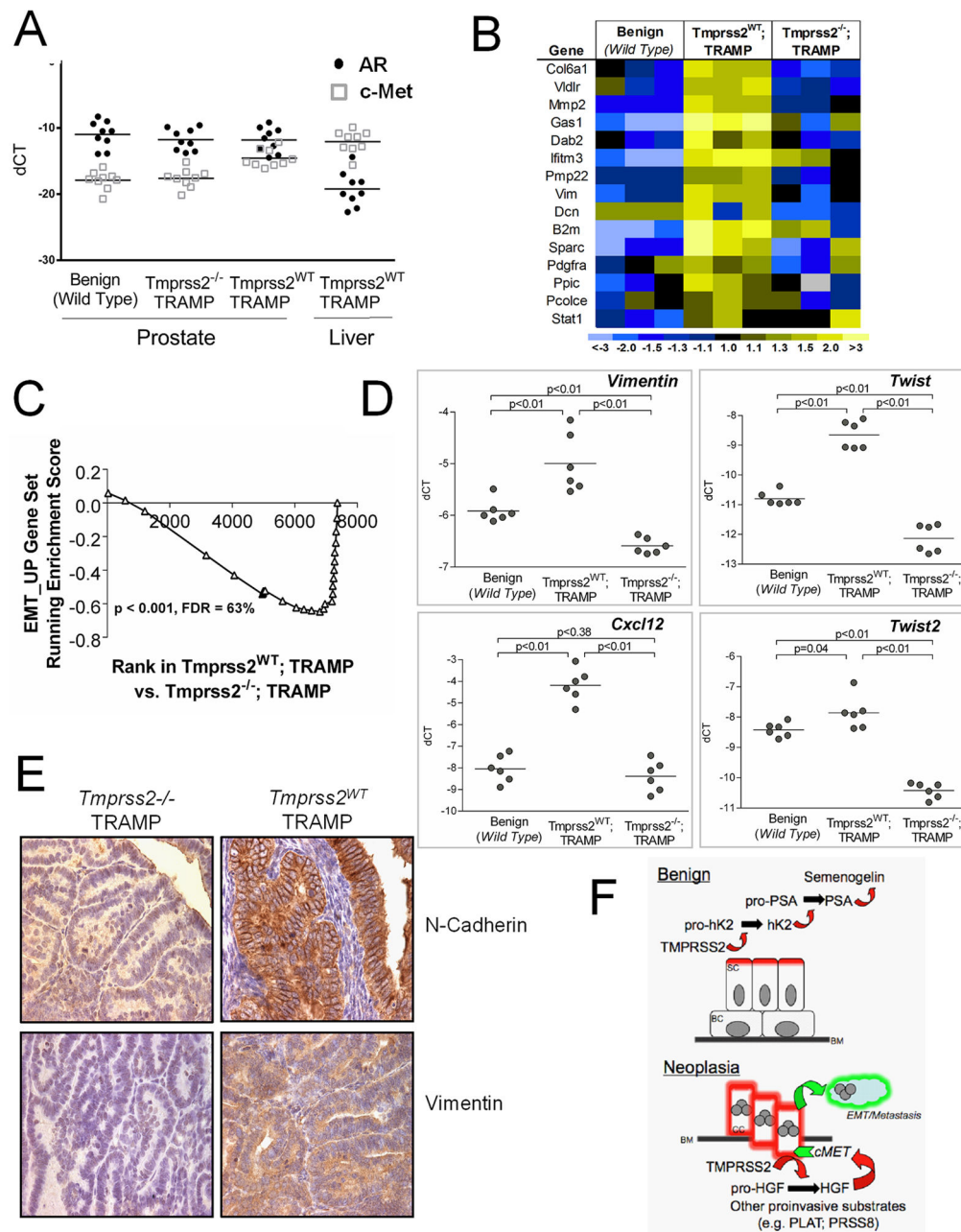
Figure 5. TMPRSS2 associates with a gene expression program involved in epithelial to mesenchymal transition (EMT)

(A) AR and c-Met transcript levels in primary and metastatic TRAMP tumors determined by qRT-PCR. **(B)** Transcript profiling of mRNAs from microdissected prostate epithelium. Genes associated with EMT are elevated in *Tmprss2^{WT}*; TRAMP tumors (yellow) and decreased in *Tmprss2^{−/−}*; TRAMP tumors (blue). **(C)** Gene set enrichment analysis (GSEA) confirms a significant enrichment in EMT-associated genes in *Tmprss2^{WT}*; TRAMP tumors ($p<0.001$). **(D)** qRT-PCR quantitation of gene expression from benign and neoplastic epithelium microdissected from TRAMP mouse strains with and without Tmprss2 activity. **(E)** Immunohistochemical staining of TRAMP tumors for EMT-associated proteins

vimentin and N-cadherin. **(F)** Schematic view of the proteolytic cascades influenced by TMPRSS2 in the context of normal physiology in benign epithelium and in neoplasia where substrates normally confined to the stroma are available for interactions with the TMPRSS2 protease. SC, secretory epithelial cell; BC, basal epithelial cell; BM, basement membrane; CC, cancerous epithelial cell, EMT, epithelial to mesenchymal transition.
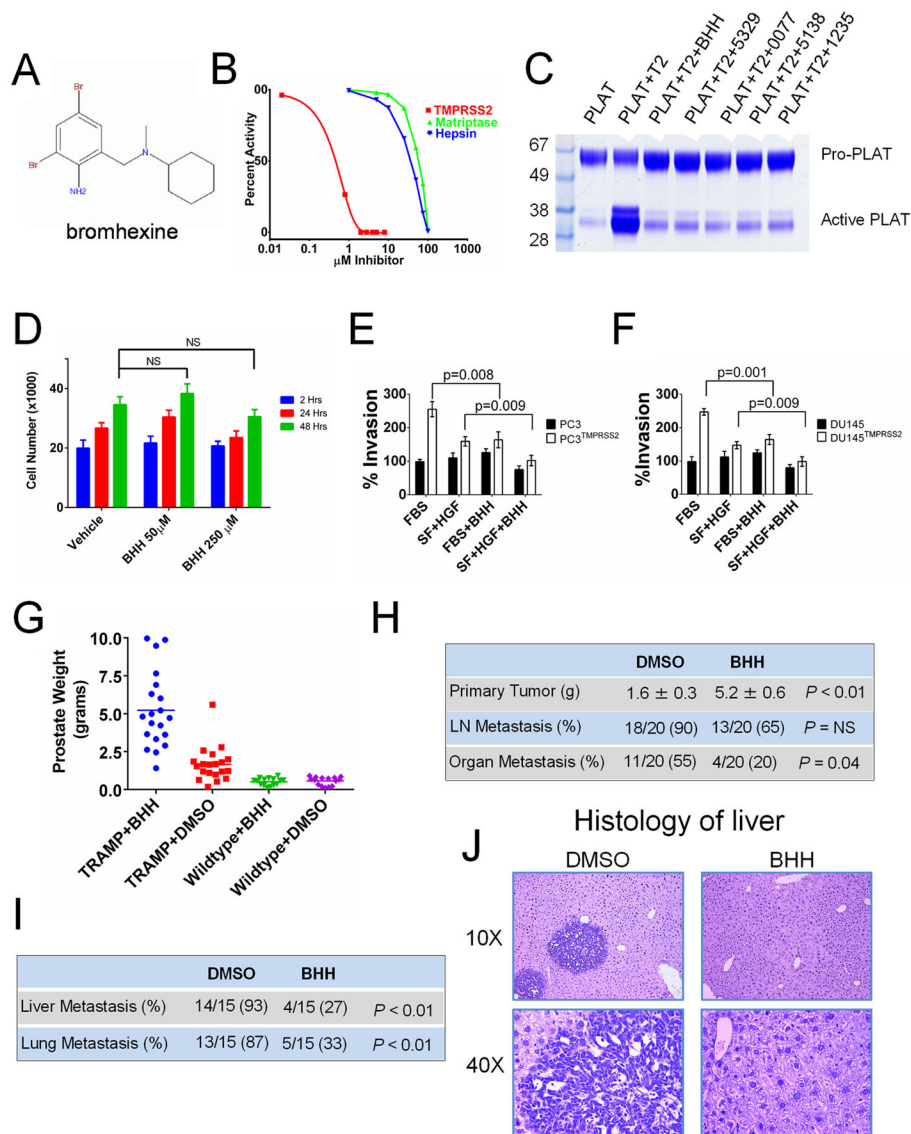
Figure 6. TMPRSS2 chemical inhibitors suppress prostate tumor growth and metastasis in vivo
(**A**) Chemical structure of the identified TMPRSS2 inhibitor bromhexine (BHH).(**B**) BHH exhibits substantially greater inhibitory activity toward TMPRSS2 relative to hepsin or matriptase. Optimal peptide substrates were used for each enzyme and substrate concentrations were determined after 30 minutes.(**C**) Suppression of TMPRSS2-induced cleavage of the TMPRSS2 substrate pro-PLAT by the chemical TMPRSS2 inhibitors identified through screening chemical libraries. T2 is active TMPRSS2. BHH is bromhexine. (**D**) BHH exposure does not induce cell death or substantially suppress the growth of DU145 cells. BHH suppresses the serum- and HGF-mediated invasion of (**E**) DU145 and (**F**) PC3 cells expressing TMPRSS2. (**G**) *In vivo* treatment with BHH increases the size of primary TRAMP tumors compared to TRAMP mice treated with DMSO vehicle. Treatment was initiated at age 15 weeks and tumor weights were determined after 20 weeks of treatment.(**H**) TRAMP mice treated with BHH have substantially fewer spontaneous

metastasis to lung or liver. **(I)** BHH treatment substantially reduced the frequency of distant metastasis following tail vein injections of tumor cells harvested from primary TRAMP tumors. **(J)** Representative histology of murine liver 8 weeks following the intravenous injection of TRAMP tumor cells showing liver metastasis in mice treated with DMSO vehicle and normal liver histology without metastasis in BHH treated mice.

Table 1

Influence of Tmprss2 expression on the frequency of prostate cancer metastasis.

Donor Age (weeks)	Donor Genotype (# donors)		Recipients with Metastases[1]		
			Liver	Lung	
12	Tmprss2+/+ TRAMP	(n=2)	0/9	0/9	p= ns[2]
	Tmprss2−/− TRAMP	(n=1)	0/3	0/3	
20	Tmprss2+/+ TRAMP	(n=2)	9/9	7/9	p< 0.001
	Tmprss2−/− TRAMP	(n=4)	0/15	0/15	
32	Tmprss2+/+ TRAMP	(n=5)	21/21	19/21	p< 0.001
	Tmprss2−/− TRAMP	(n=6)	0/28	0/28	

[1] Number of recipient mice with metastasis/number of total recipient mice

[2] Comparison of the frequency of metastasis between donor genotypes